Do mice bred selectively for high locomotor activity have a greater reliance on lipids to power submaximal aerobic exercise?

Nicole M. Templeman, Heidi Schutz, Theodore Garland, Jr and Grant B. McClelland

Am J Physiol Regul Integr Comp Physiol 303:R101-R111, 2012. First published 9 May 2012;
doi: 10.1152/ajpregu.00511.2011

You might find this additional info useful...

This article cites 50 articles, 27 of which you can access for free at:
http://ajpregu.physiology.org/content/303/1/R101.full#ref-list-1

Updated information and services including high resolution figures, can be found at:
http://ajpregu.physiology.org/content/303/1/R101.full

Additional material and information about ***American Journal of Physiology - Regulatory, Integrative and Comparative Physiology*** can be found at:
http://www.the-aps.org/publications/ajpregu

This information is current as of September 18, 2012.

American Journal of Physiology - Regulatory, Integrative and Comparative Physiology publishes original investigations that illuminate normal or abnormal regulation and integration of physiological mechanisms at all levels of biological organization, ranging from molecules to humans, including clinical investigations. It is published 24 times a year (twice monthly) by the American Physiological Society, 9650 Rockville Pike, Bethesda MD 20814-3991. Copyright © 2012 the American Physiological Society. ESSN: 1522-1490. Visit our website at http://www.the-aps.org/.

Do mice bred selectively for high locomotor activity have a greater reliance on lipids to power submaximal aerobic exercise?

Nicole M. Templeman,[1] Heidi Schutz,[2] Theodore Garland, Jr.,[2] and Grant B. McClelland[1]

[1]*Department of Biology, McMaster University, Hamilton, Ontario, Canada; and* [2]*Department of Biology, University of California Riverside, Riverside, California*

Submitted 12 September 2011; accepted in final form 7 May 2012

Templeman NM, Schutz H, Garland T, Jr, McClelland GB. Do mice bred selectively for high locomotor activity have a greater reliance on lipids to power submaximal aerobic exercise?. *Am J Physiol Regul Integr Comp Physiol* 303: R101–R111, 2012. First published May 9, 2012; doi:10.1152/ajpregu.00511.2011.—Patterns of fuel use during locomotion are determined by exercise intensity and duration, and are remarkably similar across many mammalian taxa. However, as lipids have a high yield of ATP per mole and are stored in large quantities, their use should be favored in endurance-adapted animals. To examine the capacity for alteration or differential regulation of fuel-use patterns, we studied two lines of mice that had been selectively bred for high voluntary wheel running (HR), including one characterized by small hindlimb muscles (HR_{mini}) and one without this phenotype (HR_{normal}), as well as a nonselected control line. We evaluated: *1*) maximal aerobic capacity ($\dot{V}O_{2\,max}$); *2*) whole body fuel use during exercise by indirect calorimetry; *3*) cardiac properties; and *4*) many factors involved in regulating lipid use. HR mice achieved an increased $\dot{V}O_{2\,max}$ compared with control mice, potentially in part due to HR cardiac capacities for metabolic fuel oxidation and the larger relative heart size of HR_{mini} mice. HR mice also exhibited enhanced whole body lipid oxidation rates at 66% $\dot{V}O_{2\,max}$, but HR_{mini}, HR_{normal}, and control mice did not differ in the proportional mix of fuels sustaining exercise (% total $\dot{V}O_2$). However, HR_{mini} gastrocnemius muscle had elevated fatty acid translocase (FAT/CD36) sarcolemmal protein and cellular mRNA, fatty acid binding protein (H-FABP) cytosolic protein, peroxisome proliferator-activated receptor (*PPAR*) α mRNA, and mass-specific activities of citrate synthase, β-hydroxyacyl-CoA dehydrogenase, and hexokinase. Therefore, high-running mouse lines had whole body fuel oxidation rates commensurate with maximal aerobic capacity, despite notable differences in skeletal muscle metabolic phenotypes.

aerobic capacity; experimental evolution; lipid oxidation; muscles

WHEN ENERGY DEMAND IS INCREASED, as during exercise, a major component of maintaining the essential balance between ATP production and utilization is the ability to select an appropriate mixture of metabolic fuels, in addition to adjusting total flux of substrates through metabolic pathways (50). In exercising mammals, the two predominant substrates sustaining energy expenditure in skeletal muscles are lipids (both intramuscular triglycerides and plasma free fatty acids) and carbohydrates (intramuscular glycogen stores and blood glucose; 50). As exercise intensity increases, carbohydrates support a greater proportion of energy expenditure, as they are capable of sustaining high ATP turnover rates (5, 9, 10, 29, 42, 50).

In fact, it has been long appreciated that exercise intensity largely influences metabolic fuel-use patterns, at least in the few mammalian species in which exercise metabolism has been studied (5, 9, 10, 29, 41). For example, the "crossover concept" describes a theory wherein a human's fuel use during exercise depends on the interaction between exercise intensity and endurance training status (5). Indeed, when energetic requirements of locomotion are adjusted according to an individual's maximal capacity for aerobic ATP supply ($\dot{V}O_{2\,max}$), a strong relationship exists between relative exercise intensity (i.e., intensity relative to $\dot{V}O_{2\,max}$) and the proportional mix of carbohydrates and lipids fueling exercise (29, 41, 50). Surprisingly, this relationship appears to be widely conserved among the mammalian species examined to date, irrespective of allometric variation or diversity in locomotor capabilities (29, 41, 50). Thus this model of mammalian fuel use represents a valuable tool to formulate hypotheses.

The underlying explanations for this evident unity in mammalian fuel-use patterns remain unknown. Likely, many factors influence the fractional contribution of carbohydrates and lipids to energy supply, including recruitment of different muscle fiber types, hormonal regulation, substrate and oxygen availability, and the regulation of enzyme and substrate transporter quantities and activities (6, 29, 31). For instance, both Roberts et al. (41) and McClelland (29) proposed that one mechanism accounting for the conservation of the fuel-use pattern may be the progressive recruitment of type IIB (fast glycolytic) muscle fibers with increasing exercise intensity (25, 44), which could be instrumental among all mammals in mediating the gradual shift of fuel preference toward carbohydrates (29, 41). However, it is currently unclear what mechanisms cause variation among mammals in absolute fuel oxidation or flux rates, or even if the mechanisms that explain the unity in proportional mix of fuels are common across taxa.

To further explore the underpinnings of the mammalian fuel-use pattern during exercise, we used a model of experimental evolution in which different breeding lines of mice have been selectively bred for high levels of voluntary wheel running (46). This allows for the controlled examination of the evolution of diverse voluntary exercise phenotypes; such models provide opportunities for empirical testing of evolutionary hypotheses without such complications as phylogenetic divergences, as occurs with interspecific comparisons (12). Mice from the high running (HR) lines voluntarily run ~170–200% more revolutions/day on running wheels than those from nonselected control lines and have a higher endurance capacity during forced treadmill exercise (13, 34). This animal model includes four replicate HR lines, providing opportunities for the development of multiple solutions (i.e., differential adaptive changes in subordinate traits) in response to a uniform selective influence (12, 14). For instance, occurrence of a "mini muscle" phenotype has increased in frequency in two of the four HR lines (12, 13). Mice with the "mini muscle" phenotype

Address for reprint requests and other correspondence: G. B. McClelland, Dept. of Biology, McMaster Univ., 1280 Main St. West, Hamilton, Ontario, L8S 4K1, Canada (e-mail: grantm@mcmaster.ca).

 0363-6119/12 Copyright © 2012 the American Physiological Society

(HR_{mini}) have a drastically reduced content of type IIB muscle fibers in their hindlimb muscles, resulting in increased mass-specific activities of aerobic enzymes and reduced mass-specific activities of anaerobic enzymes in these muscles, relative to mice with the normal muscle phenotype (3, 18, 19, 22).

In addition to the emergence of the "mini muscle" phenotype, selective breeding for high locomotor activity also led to an increased whole animal $\dot{V}O_{2\,max}$ (corrected for differences in body mass) in all HR lines (24, 38, 40, 47). Furthermore, female HR_{mini} mice achieve a greater $\dot{V}O_{2\,max}$ than HR mice with the normal muscle phenotype (HR_{normal}) but only under hypoxic conditions (38). It has been proposed that heart enlargement in HR_{mini} mice could contribute to this increased aerobic performance, especially in hypoxia (39); however, it has not yet been determined whether the hearts of selected mice show significant physical (i.e., hypertrophic) or metabolic remodeling. Therefore, one component of our investigation was to characterize physical and metabolic properties of cardiac muscle in these mice.

Lipids are highly chemically reduced, have a high yield of ATP per mole of fuel (high energy density), and in mammals, are stored in large quantities compared with carbohydrates. So, on first principles, one might predict that mice from selectively bred HR lines should rely more heavily on this fuel to power submaximal locomotion. We hypothesized that HR_{mini} mice in particular would exhibit a shift in the fuel-use pattern toward both a greater absolute lipid flux rate and an increased relative lipid contribution to total aerobic energy expenditure (measured as $\dot{V}O_2$), considering the enhanced aerobic capacity of their muscles and reduction in type IIB (fast glycolytic) muscle fibers. To test this hypothesis, we assessed whole body fuel use during submaximal exercise and examined key regulatory points of the fatty acid metabolic pathway in the gastrocnemius muscle, a major hindlimb muscle that has notable phenotypic alterations in the HR_{mini} mice (18, 19). Thus we had a unique opportunity to evaluate the effects of voluntary locomotor behavior and aerobic capacity on the mammalian fuel-use pattern without many of the complications of interspecific comparative studies by using a model of experimental evolution.

MATERIALS AND METHODS

Animals. All experimental procedures were approved by the University of California Riverside Institutional Animal Care and Use Committee, as well as by the McMaster University Animal Research Ethics Board following Canadian Council for Animal Care guidelines.

We used male mice from an animal model in which four closed lines are selectively bred for high voluntary wheel-running behavior (HR). For details about the selective breeding regimen and general husbandry, refer to Swallow et al. (46). In brief, four replicate HR lines experience within-family selection for total revolutions run on *days 5* and *6* of a 6-day period of wheel access when they are young adults. Four additional lines also receive the 6-day period of wheel access but are bred as controls without any intentional selection. Animals in our study were sampled from one control line (lab designation *line 2*), one HR_{mini} line (*line 3*), and one HR_{normal} line (*line 8*). Hearts were sampled from mice of 8- to 9-wk-old *generation 56* ($N = 30$ total). Six- to nine-week-old mice from *generation 57* were randomly distributed into two batches of five mice from each line and tested for in vivo exercise data ($N = 30$ total). For skeletal muscle measurements, gastrocnemius muscles were also sampled in two batches, using 8- to 10-wk-old nonexercised mice (no prior treadmill exposure) from *generation 57* ($N = 28$ total).

During the in vivo experiments, mice were individually housed at room temperature (~22°C) and maintained on a 12:12 h light:dark cycle, with lights on at 7:00. Water and laboratory chow (8604 Teklad rodent diet, Harlan Laboratories) were available ad libitum, except during fasting periods.

Treadmill exercise and indirect calorimetry. A positive-pressure, flow-through respirometry system was used for all measurements of rates of oxygen consumption ($\dot{V}O_2$) and carbon dioxide production ($\dot{V}CO_2$) at room temperature (~22–25°C). Animals were exercised on a custom-built motorized treadmill at an incline of 10°, enclosed in a Plexiglas metabolic chamber (approximate volume 800 ml) and equipped with stimulus electrical grid. Air entering the chamber was scrubbed of H_2O by Drierite (W. A. Hammond Drierite, Xenia, OH) and of CO_2 by soda lime and Ascarite (Fisher Scientific, Pittsburgh, PA) and maintained at a constant flow of 2,000 ml/min by combined pump and mass-flow controller unit (MFS, Sable Systems International, Las Vegas, NV). Treadmill chamber air was subsampled at 200 ml/min and scrubbed of H_2O by magnesium perchlorate (Fisher Scientific), and then passed through an O_2 and CO_2 analyzer (FoxBox portable analysis instrument; Sable Systems International). Data were collected with data acquisition software (Expedata; Sable Systems International) at a frequency of 1 sample/s. The accuracy of this setup was determined by measuring the combustion of methanol as described previously (31) and found to be ±5% of theoretical values for absolute rates of $\dot{V}O_2$ and $\dot{V}CO_2$ and ±1% of theoretical values for respiratory exchange ratio ($RER = \dot{V}CO_2/\dot{V}O_2$). Before $\dot{V}O_{2\,max}$ trials, mice were familiarized with forced treadmill running for 10–15 min on 2 consecutive days. For all exercise trials, mice had a 5-min adjustment period in the chamber before exercise began with a starting speed of 10 or 13 m/min and incrementally increased by 3 m/min every 1–2 min. After correction for any baseline drift in incurrent O_2 or CO_2 during the run, 10–15 s of data at the plateau of $\dot{V}O_2$ during the 1–2 min of each speed was used for the assessment of $\dot{V}O_2$ values. $\dot{V}O_{2\,max}$ was defined as the maximal steady-state interval at which at least two of the following criteria were satisfied: *1*) no change in $\dot{V}O_2$ with increasing speed, *2*) $RER \geq 1.0$, and *3*) the mouse no longer maintained position on the treadmill (24, 31, 38, 43, 47). Trial quality was also assessed subjectively by assigning a score between 1 and 5 (47), and runs deemed unacceptable (scores below 3) were repeated. There was a minimum of 24 h between exercise bouts for any individual.

For all submaximal exercise trials, mice were fasted 6–8 h to ensure a postabsorptive state. The order of the two submaximal exercise intensity trials (target 60% $\dot{V}O_{2\,max}$ and 80% $\dot{V}O_{2\,max}$, on average 66% $\dot{V}O_{2\,max}$ and 78% $\dot{V}O_{2\,max}$, designated as "low-intensity" and "high-intensity" exercise, respectively) was randomized for each mouse, and the trials were performed between 13:00 and 19:00. Initial treadmill speed for submaximal exercise tests was determined from the relationship between speed and $\dot{V}O_2$ during the $\dot{V}O_{2\,max}$ trials; minor adjustments to treadmill speed were made based on real-time monitoring of $\dot{V}O_2$ to maintain a constant relative intensity. Sixty seconds of continuous data from between *minutes 9* to *11* of each individual trial were used for analyses. Rates of $\dot{V}CO_2$ and $\dot{V}O_2$ (ml/h) were calculated using *Eq. 3b* from Withers (52). Lipid and carbohydrate oxidation rates were estimated using indirect calorimetry (11), and estimations were based on the assumption that protein contributions to total oxidation were negligible during aerobic exercise in a postabsorptive state (37). The proportional contribution of lipids or carbohydrates to whole body oxidation was determined by dividing the estimated lipid or carbohydrate oxidation rate (in μmol $O_2 \cdot h^{-1} \cdot g^{-1}$) by the measured total rate of oxygen consumption during the exercise bout ($\dot{V}O_2$, in μmol·O_2 $h^{-1} \cdot g^{-1}$).

Tissue sampling. All tissue sampling took place between 13:00 and 18:00 h. Nonexercised mice from *generation 57* were fasted for 6–8 h before euthanasia via decapitation. The left and right gastrocnemius

muscles were removed, weighed, and flash frozen in dry ice with aluminum clamps. The left and right ventricles were separated and sampled in a similar manner from a separate group of mice (*generation 56*) that were not fasted before euthanization. All tissues were powdered in liquid nitrogen with a mortar and pestle and stored at −80°C until used.

Enzyme activity assays. For all assays, chemicals were purchased from Sigma-Aldrich (Oakville, ON, Canada), unless otherwise indicated. Maximal activities (V_{max}) of β-hydroxyacyl-CoA dehydrogenase (HOAD), hexokinase (HK), carnitine palmitoyltransferase II (CPT II), and citrate synthase (CS) were measured in left ventricles and right gastrocnemius muscles, following previously described procedures (21, 28) with slight modifications. Powdered tissue was diluted 1:20 (mg tissue:μl) with ice-cold extraction buffer (in mM: 100 K_2HPO_4/KH_2PO_4, 5 EDTA, 0.1% Triton X-100, pH 7.6) and homogenized with a cooled glass on glass homogenizer.

Maximal HOAD activity was assayed at 340 nm in assay buffer in mM: 100 TEA-HCl (pH 7.0), in the presence of 0.28 NADH and 5 EDTA, with 0.1 acetoacetyl-CoA added as substrate. Maximal HK activity, assayed at 340 nm, was measured using 50 HEPES as the buffer (pH 7.6), in the presence of 8 $MgCl_2$, 0.5 NADP, 8 ATP, and excess levels of glucose-6-phosphate dehydrogenase (4 U), with 5 glucose added as substrate. Maximal CS activity, measured at 412 nm, was assayed in 100 Tris·HCl (pH 8.0) in the presence of 0.1 2,2′-nitro-5,5′-dithiobenzoic acid (DTNB) and 0.3 acetyl-CoA, with 0.25 oxaloacetate added as substrate. Maximal CPT II activity, measured at 412 nm, was assayed in 40 Tris·HCl (pH 8.0) in the presence of 0.2 DTNB, 1.5 EDTA, and 0.05 palmitoyl-CoA, with 5 L-carnitine added as substrate. This assay is believed to measure CPT II activity because CPT I is detergent labile (see Ref. 32).

All maximal enzyme activity levels were assayed at 37°C using a SpectraMax Plus 384 spectrophotometer (Molecular Devices). Assays were performed in triplicate, with an additional negative control well (lacking substrate) to correct for background activity. Enzyme activity data are presented as the mean rate of conversion of substrate to product (Unit = μmol/min).

DNA quantification. Total DNA content was quantified in the left ventricles (48), in tissue homogenates used for the enzyme activity assays, after they were frozen and rethawed, and further diluted to 1:40 (mg tissue:μl extraction buffer). In brief, aliquots of tissue homogenates in 2× digestion buffer (in mM: 100 NaCl, 10 Tris·HCl, 25 EDTA, 0.5% SDS, 0.2 mg/ml proteinase K, pH 8.0) were digested overnight (18 h) at 55°C. Digested samples were incubated with PicoGreen, and fluorescence was measured (excitation 480 nm, emission 535 nm) by a SpectraMax Gemini XPS fluorescence spectrophotometer (Molecular Devices) and compared with a DNA standard curve (48).

Sample preparation for immunoblotting and ELISA. The cytosolic and sarcolemmal fractions of left gastrocnemius tissue were prepared as previously described (7, 30), with slight modifications. Powdered tissue was homogenized with a cooled glass on glass homogenizer in a buffer containing (in mM): 30 HEPES, 210 sucrose, 2 EGTA, 40 NaCl, and a protease inhibitor cocktail (Complete MINI, Roche Diagnostics), at pH 7.4. The homogenate was centrifuged at 600 *g* for 10 min at 4°C, and the supernatant from this step was then centrifuged at 10,000 *g* for 20 min at 4°C. The ensuing supernatant was diluted (0.75 × volume) with a buffer containing 1.167 M KCl and 58.3 mM Na_4PPi at pH 7.4 and centrifuged at 230,000 *g* for 2 h at 4°C. The resulting supernatant was collected as the cytosolic fraction. The pellet was resuspended in a buffer containing 10 mM Tris and 1 mM EDTA, at pH 7.4. This suspension was mixed with 16% SDS (0.33 × volume) and centrifuged at 1,100 *g* for 20 min at room temperature, with the ensuing supernatant collected as the sarcolemmal fraction. Total protein content in cytosol and sarcolemmal samples was quantified with the commercial Pierce BCA Protein Assay kit (Thermo Scientific, Whitby, ON, Canada).

Immunoblotting. Fatty acid translocase (FAT/CD36) protein content was measured in sarcolemmal fractions from gastrocnemius muscles using a commercial CD36 (H-300) antibody and a horseradish peroxidase-linked anti-rabbit secondary antibody (sc-9154 and sc-2313, respectively; Santa Cruz Biotechnology, Santa Cruz, CA). Equal amounts of total sarcolemmal protein (5 μg/lane) were separated by electrophoresis in 10% polyacrylamide gels (Bio-Rad Laboratories, Mississauga, ON, Canada). Protein was transferred to polyvinylidene difluoride membranes (Bio-Rad Laboratories) and blocked with 5% bovine serum albumin (BSA) dissolved in PBS-T (in mM: 1.5 $NaH_2PO_4·H_2O$, 8.1 Na_2HPO_4, 145.4 NaCl, 0.05% Tween 20, pH 7.4) overnight at 4°C. Membranes were washed with 1% BSA/PBS-T (2 × 5 min), and then primary antibody (diluted 1:200 in 1% BSA/PBS-T) for 1 h, 1% BSA/PBS-T (1 × 15 min, 3 × 5 min), secondary antibody (diluted 1:5,000 in 1% BSA/PBS-T) for 1 h, and, lastly, 1% BSA/PBS-T (1 × 15 min, 3 × 5 min). Chemiluminescence (Perkin Elmer, Waltham, MA) was detected on autoradiographic films (Kodak XAR). Relative protein levels were evaluated based on the measure of band volumes, determined using ImageJ software. All samples are expressed normalized against a standard sample (a mixture of sarcolemmal protein pooled from all three mouse lines) that was loaded onto each gel.

H-FABP ELISA. Heart-type fatty acid binding protein (H-FABP) content was determined in cytosolic fractions of gastrocnemius muscles, using an enzyme-linked immunosorbent assay (ELISA) based on the sandwich principle. Equal amounts of total cytosolic protein (0.015 μg) were assayed for each sample, using a commercial ELISA kit designed for mouse H-FABP (HK403; Hycult Biotech). H-FABP protein levels are expressed relative to total cytosolic protein content.

Real-time PCR. Real-time PCR was used for the relative quantification of peroxisome proliferator-activated receptor (*PPAR*)-α, medium-chain acetyl-CoA dehydrogenase (*MCAD*), and muscle- and liver-type *CPT-1* (*Cpt-1β* and *Cpt-1α*, respectively) mRNA levels in the right and left ventricles, using TATA-binding protein (*TBP*) as the housekeeping gene. Relative quantification of *PPARα*, peroxisome proliferator-activated receptor gamma coactivator 1-α (*PGC-1α*), *PPARβ/δ*, NAD-dependent deacetylase sirtuin-1 (*SIRT1*), and *FAT/CD36* was performed in the left gastrocnemius muscles, using *18S* as the housekeeping gene. Primer sequences (Table 1) were either previously published (1, 48) or designed using Primer 3 software. The specificity of the resulting primer pairs (Mobix, Hamilton, ON, Canada) was tested separately for each mouse line, using PCR and gel electrophoresis.

RNA was extracted by homogenization with TRIzol reagent (Invitrogen, Burlington, ON, Canada), based on the acid guanidinium thiocyanate-phenol-chloroform extraction method. Total RNA concentration was measured at 260 nm using a NanoDrop ND-1,000 spectrophotometer (Fisher Scientific). To generate cDNA, 1 μg of total RNA was treated with DNase I (Invitrogen), and reverse transcription was carried out by SuperScript II RNase H^- reverse transcriptase (Invitrogen) as previously described (48).

Five microliters of 1:5 (cDNA:μl water) diluted cDNA were mixed with 12.5 μl SYBR green (Bio-Rad), 5.5 μl RNase/DNase-free water, and 1 μl each of forward and reverse primers (5 μM) for quantitative real-time PCR reactions. A negative control of water was run on each plate to ensure a lack of contamination. Reactions were performed in duplicate on a Stratagene MX3000P QPCR system (Stratagene, La Jolla, CA), using SYBR green with ROX as the reference dye. In all cases, the thermal program consisted of a 3-min initial denaturation at 95°C, then 40 cycles of 95°C for 15 s, 60°C for 45 s, and 72°C for 30 s. A dissociation curve analysis was performed to verify the specificity of PCR products. The relative mRNA levels of each sample were calculated using the comparative C_t method (8). All values are normalized against mRNA levels of the housekeeping gene, which did not differ between groups ($P > 0.2$ for each housekeeping gene). Statistical analyses for gene expression were performed on values normalized to the housekeeping gene, but for the purpose of data

Table 1. *Primer sequences used for real-time PCR mRNA quantification*

Gene	Forward Primer (5′-3′)	Reverse Primer (5′-3′)
*Cpt-1α**	AAACCCACCAGGCTACAGTG	TCCTTGTAATGTGCGAGCTG
*Cpt-1β**	CCCATGTGCTCCTACCAGAT	CCTTGAAGAAGCGACCTTTG
FAT/CD36	CAACTGGTGGATGGTTTCCT	GCAGAATCAAGGGAGAGCAC
*MCAD**	TCGGAGGCTATGGATTCAAC	TCAATGTGCTCACGAGCTATG
PGC-1α	ATGTGTCGCCTTCTTGCTCT	ATCTACTGCCTGGGGACCTT
*PPARα**	TCATACATGACATGGAGACCTTG	ACTGGCAGCAGTGGAAGAATC
PPARβ/δ	GGTAGAAGCCATCCAGGACA	CCGTCTTCTTTAGCCACTGC
SIRT1†	GATACCTTGGAGCAGGTTGC	CTCCACGAACAGCTTCACAA
*TBP**	GGCCTCTCAGAAGCATCACTA	GCCAAGCCCTGAGCATAA
18S	TGTGGTGTTGAGGAAAGCAG	TCCCATCCTTCACATCCTTC

*From Templeman et al. (48). †From Asher et al. (1). See text for definitions of abbreviations.

presentation, these normalized values are expressed relative to mean control values (arbitrarily set at 1.0).

Statistics. Statistical analyses were performed using SPSS 11.0 software. Analysis of covariance (ANCOVA) models were used for each dependent variable. Body mass was always included as a covariate, except when it had been accounted for in the dependent variable, or when examining raw ventricular masses independent of body mass. Analyses of FAT/CD36 and H-FABP protein, maximal enzyme activity, and mRNA content were also performed without body mass as a covariate (21, 22), and this did not alter results in most cases. Age and batch were also tested as covariates and were removed from the model when they had no significant effects. To account for individual variation during exercise bouts, the covariate of "relative exercise intensity" (i.e., $\dot{V}O_2$ relative to individual $\dot{V}O_{2\,max}$) was included in the ANCOVA models for fuel oxidation rates and proportional contributions to total oxidation.

For analyses in which a significant effect was detected, pairwise comparisons with a Bonferroni correction were used to compare mouse phenotypes. For all statistical analyses, tests were two-tailed and the critical α-level was set at $P = 0.05$.

RESULTS

In vivo: $\dot{V}O_{2\,max}$ and fuel use during exercise. Both lines of HR mice exhibited a greater $\dot{V}O_{2\,max}$ than nonselected control mice, regardless of whether $\dot{V}O_{2\,max}$ was analyzed as a mass-specific variable, or alternately, as a whole animal value with the covariate of body mass ($P < 0.05$; Fig. 1, Table 2). Moreover, the mass-specific $\dot{V}O_{2\,max}$ of HR_{mini} mice was elevated compared with HR_{normal} mice ($P < 0.05$; Table 2). However, when $\dot{V}O_{2\,max}$ was analyzed as whole animal values with body mass as a covariate, the difference between HR_{mini} and HR_{normal} mice was not statistically significant. The estimated marginal mean whole animal $\dot{V}O_{2\,max}$ and SE for control, HR_{mini}, and HR_{normal} mice were 4.353 ± 0.058, 4.933 ± 0.059, and 4.794 ± 0.057 ml/min, respectively, as evaluated at an average body mass of 28.1 g (Fig. 1).

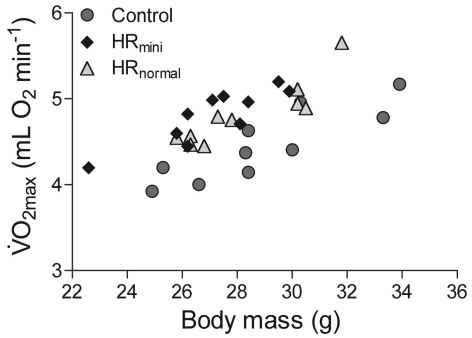

Fig. 1. Individual whole animal maximal aerobic capacity ($\dot{V}O_{2\,max}$) of control mice and mice selectively bred high voluntary wheel running (HR) characterized by small hindlimb muscles (HR_{mini}) and without this phenotype (HR_{normal}), presented across the range of body masses ($n = 9$–10).

During low-intensity exercise (66 ± 1% for controls, 64 ± 1% for HR_{mini} mice, and 69 ± 2% $\dot{V}O_{2\,max}$ for HR_{normal} mice; overall average 66% $\dot{V}O_{2\,max}$; Table 2), the greater total $\dot{V}O_2$ of HR mice (Table 2) was primarily supplied by an increased flux of lipids; HR_{mini} mice exhibited higher absolute rates of lipid oxidation than control mice, a difference that approached significance for HR_{normal} mice as well ($P < 0.05$ for HR_{mini} mice, $P = 0.057$ for HR_{normal} mice; Table 2). Although the concurrent rates of carbohydrate oxidation were not significantly different among the three mouse phenotypes (Table 2), there were no statistically significant differences in the proportional mix of fuels supplying oxidation at 66% $\dot{V}O_{2\,max}$ when fuel oxidation rates were expressed relative to total $\dot{V}O_2$ (Fig. 2*A*). For all mice, ~70% of energy was supplied via the oxidation of lipids, with the remaining 30% by the oxidation of carbohydrates (Fig. 2*A*).

During high-intensity exercise (78 ± 1% $\dot{V}O_{2\,max}$ for controls, 76 ± 1% $\dot{V}O_{2\,max}$ for HR_{mini} mice, and 79 ± 1% $\dot{V}O_{2\,max}$ for HR_{normal} mice; overall average 78% $\dot{V}O_{2\,max}$; Table 2), the absolute lipid and carbohydrate oxidation rates in control mice were equivalent to those in HR mice (Table 2). At this increased intensity, carbohydrates contributed more than 40% toward total oxidation in all mice (Fig. 2*B*).

Cardiac properties. Relative to body mass, HR_{mini} mice had significantly larger left ventricles than both control and HR_{normal} mice ($P \leq 0.001$; Table 3). This was principally due to a reduced body mass in HR_{mini} mice compared with the other two lines ($P < 0.05$; Table 3); however, a slight enlargement of whole ventricle mass in HR_{mini} mice approached statistical significance even without the inclusion of body mass as a covariate ($P = 0.096$; Table 3). There were no statistical differences in left ventricle DNA content, whether expressed per gram wet mass or per whole ventricle (Table 3).

In addition to physical changes, both lines of HR mice exhibited some degree of cardiac metabolic remodeling compared with control mice, as indicated by increased maximal HK activity concurrent to reduced maximal CPT II activity ($P < 0.05$; Fig. 3). However, there were no statistically significant differences in the mRNA content of *PPARα*, *MCAD*, *CPT-1α*, or *CPT-1β* in either the right or left ventricles of HR_{mini}, HR_{normal}, or control mice (Table 4).

Skeletal muscle FAT/CD36 and H-FABP. The skeletal muscle of nonexercised HR_{mini} mice was characterized by a mark-

Table 2. *Mass-specific $\dot{V}O_{2max}$ and whole body lipid and carbohydrate oxidation rates of control, HR_{mini}, and HR_{normal} mice during low- and high-intensity submaximal exercise*

	Control mice	HR_{mini} Mice	HR_{normal} Mice
Mass-specific $\dot{V}O_{2max}$, ml $O_2 \cdot h^{-1} \cdot g^{-1}$	9.26 ± 0.12[a] (10)	10.63 ± 0.12[b] (10)	10.18 ± 0.13[c] (9)
66% VO_{2max}			
Exercise intensity, % $\dot{V}O_{2max}$	66 ± 1 (10)	64 ± 1 (10)	69 ± 2 (9)
$\dot{V}O_2$, ml $O_2 \cdot h^{-1} \cdot g^{-1}$	6.14 ± 0.09[a] (10)	7.04 ± 0.09[b] (10)	6.84 ± 0.10[b] (9)
$\dot{V}CO_2$, ml $CO_2 \cdot h^{-1} \cdot g^{-1}$	4.93 ± 0.08[a] (10)	5.54 ± 0.09[b] (10)	5.37 ± 0.09[b] (9)
Lipid oxidation, ml $O_2 \cdot h^{-1} \cdot g^{-1}$	4.12 ± 0.23[a] (10)	5.09 ±0.24[b] (10)	4.97 ± 0.25[b]* (9)
Carbohydrate oxidation, ml $O_2 \cdot h^{-1} \cdot g^{-1}$	2.02 ± 0.20 (10)	1.95 ± 0.21 (10)	1.85 ± 0.23 (9)
78% $\dot{V}O_{2max}$			
Exercise intensity, % $\dot{V}O_{2max}$	78 ± 1 (10)	76 ± 1 (9)	79 ± 1 (9)
$\dot{V}O_2$, ml $O_2 \cdot h^{-1} \cdot g^{-1}$	7.22 ± 0.09[a] (10)	8.21 ± 0.11[b] (9)	8.00 ± 0.10[b] (9)
$\dot{V}CO_2$, ml $CO_2 \cdot h^{-1} \cdot g^{-1}$	5.93 ± 0.12[a] (10)	6.88 ± 0.14[b] (9)	6.73 ± 0.14[b] (9)
Lipid oxidation, ml $O_2 \cdot h^{-1} \cdot g^{-1}$	4.39 ± 0.33 (10)	4.53 ± 0.37 (9)	4.32 ± 0.37 (9)
Carbohydrate oxidation, ml $O_2 \cdot h^{-1} \cdot g^{-1}$	2.83 ± 0.32 (10)	3.68 ± 0.37 (9)	3.67 ± 0.36 (9)

Mass-specific maximal aerobic capacity ($\dot{V}O_{2max}$) is presented as estimated marginal means ± SE, as adjusted for the cofactor of group batch. Exercise intensities (% $\dot{V}O_{2max}$) are presented as simple means ± SE. All mass-specific oxidation rates are presented as estimated marginal means ± SE, as adjusted for the covariate of individual % $\dot{V}O_{2max}$. Sample size is shown in parenthesis for each trait. The presence of letters denotes statistical significance, where values not sharing a common letter are significantly different from each other ($P < 0.05$, except an * indicates $P = 0.057$). See text for definitions of abbreviations.

edly enhanced capacity for fatty acid uptake and intracellular transport. Both *FAT/CD36* mRNA levels and FAT/CD36 sarcolemmal protein content was nearly threefold higher in the gastrocnemius of HR_{mini} mice than in mice with the normal muscle phenotype ($P < 0.05$; Fig. 4). Additionally, HR_{mini} mice had nearly double the amount of cytosolic H-FABP protein (per mg total cytosolic protein) of HR_{normal} or control mice in the gastrocnemius ($P < 0.05$; Fig. 5).

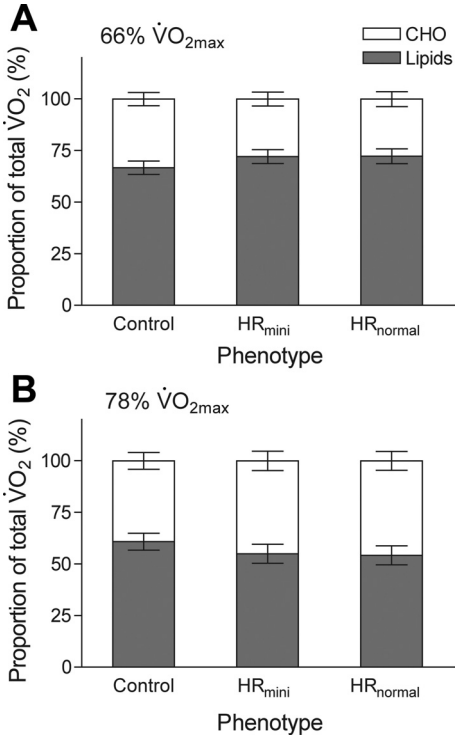

Fig. 2. Proportional contributions to whole body oxidation rates by carbohydrates and lipids, at average exercise intensities of 66% $\dot{V}O_{2\,max}$ (*A*) and 78% $\dot{V}O_{2\,max}$ (*B*) in control mice and selectively bred HR_{mini} and HR_{normal} mice ($n = 9$–10). Data are presented as estimated marginal means ± SE, as adjusted for the covariate of individual relative exercise intensity.

Skeletal muscle metabolic enzyme activities. The mass-specific maximal activities of CS, HOAD, and HK were greatly augmented in the gastrocnemius of HR_{mini} mice compared with mice with a normal muscle phenotype ($P < 0.05$; Fig. 6*A*). In fact, because mass-specific enzyme activities nearly double those of control mice (Fig. 6*A*), in a gastrocnemius less than half the mass ($P < 0.05$; Table 3), for these enzymes HR_{mini} mice had equivalent total maximal activities as control mice when expressed per whole muscle (Fig. 6*B*). The mass-specific maximal CPT II activity was not significantly different between HR_{mini} and control mice, as reflected in the reduced whole muscle maximal CPT II activity in the mini muscles (Fig. 6).

Conversely, although HR_{normal} mice did not have altered mass-specific enzyme activities compared with control mice, on a whole muscle basis they exhibited significantly greater maximal activities of CS, HOAD, CPT II, and HK ($P < 0.05$; Fig. 6*B*). These differences were also significant with body mass as a covariate (data not shown). The elevation in total muscle metabolic enzyme activity was likely reflective of a slightly increased gastrocnemius mass in HR_{normal} mice, which approached statistical significance ($P = 0.053$; Table 3). HR_{normal} whole muscle CS, CPT II, and HK maximal activities were significantly elevated above those of HR_{mini} mice as well ($P < 0.05$; Fig. 6*B*).

Skeletal muscle gene expression and transcriptional regulation. mRNA levels of *PGC-1α*, *PPARβ/δ*, and *SIRT1* were not significantly different among phenotypes, but *PPARα* mRNA content was ~2.5-fold greater in the resting gastrocnemius of HR_{mini} mice than in HR_{normal} or control mice ($P < 0.05$; Fig. 7*A*). Furthermore, transcript levels of the PPAR-regulated gene *FAT/CD36* were closely correlated with *PPARα* among all mice ($r = 0.92$, $p \leq 0.001$; Fig. 7*B*).

DISCUSSION

Our primary goal was to determine whether mice selectively bred for high voluntary running have greater whole body absolute lipid oxidation rates during exercise and a greater contribution of lipids to total aerobic energy expenditure. Our results indicate that selective breeding for high voluntary

Table 3. *Physical and cardiac characteristics of control, HR_{mini}, and HR_{normal} mice*

	Control Mice	HR_{mini} Mice	HR_{normal} Mice
Body mass, g	29.8 ± 0.6[a] (20)	27.5 ± 0.6[b] (18)	30.1 ± 0.5[a] (20)
Gastrocnemius mass, mg	123 ± 3[a] (20)	64 ± 3[b] (17)	132 ± 3[a] (20)
Left ventricle mass, mg	104.2 ± 2.9 (10)	110.9 ± 2.1 (10)	105.0 ± 3.8 (10)
Right ventricle mass, mg	20.2 ± 0.8 (10)	22.5 ± 1.0 (10)	21.8 ± 1.3 (10)
Ventricular mass, mg	124.4 ± 2.8 (10)	133.4 ± 2.7 (10)	126.8 ± 3.1 (10)
Relative left ventricle mass, mg/g body mass	3.24 ± 0.07[a] (10)	3.68 ± 0.06[b] (10)	3.29 ± 0.06[a] (10)
Relative right ventricle mass, mg/g body mass	0.63 ± 0.02 (10)	0.75 ± 0.04 (10)	0.70 ± 0.06 (10)
Relative ventricular mass, mg/g body mass	3.87 ± 0.06[a] (10)	4.43 ± 0.09[b] (10)	3.99 ± 0.08[a] (10)
Left ventricle DNA, mg/g wet mass	5.59 ± 0.42 (8)	5.65 ± 0.38 (8)	4.99 ± 0.43 (8)
Total left ventricle DNA, mg/left ventricle	0.60 ± 0.05 (8)	0.62 ± 0.04 (8)	0.50 ± 0.06 (8)

Data are presented as simple means ± SE, with the exception of gastrocnemius muscle mass, which is presented as estimated marginal means ± SE as adjusted for the covariate of body mass. Sample size is shown in parenthesis for each trait. The presence of letters denotes statistical significance, where values not sharing a common letter are significantly different from each other ($P < 0.05$).

exercise leads to an increase in the absolute rate of lipid oxidation when individuals exercise at the same relative intensity. These oxidation rates are scaled with increases in maximal aerobic capacity in both HR_{normal} and HR_{mini} mice, resulting in the proportional contributions by lipids and carbohydrates to total exercise energy expenditure being equal among all mice. The two selectively bred HR lines examined showed distinct capacities in the gastrocnemius muscle for cellular lipid uptake (FAT/CD36), cytosolic transport (H-FABP), and mitochondrial oxidation (enzyme V_{max}), suggesting that in these distinct high-running phenotypes, the response to selective breeding may have targeted different mechanisms to enhance lipid oxidation rates (e.g., capacity for oxidation of circulatory versus intramuscular sources) over that of the control line.

Aerobic capacity and cardiac properties. Our study not only confirms a 10–14% rise in $\dot{V}O_{2\,max}$ in HR mice (24, 38, 40, 47) but also indicates that *generation 57* HR_{mini} mice achieve a greater mass-specific $\dot{V}O_{2\,max}$ than HR_{normal} mice (at least the *line 8* studied here), although this difference was not significantly different on a whole animal $\dot{V}O_{2\,max}$ basis with body mass as a covariate. Previous studies indicated that the physiological constraints of $\dot{V}O_{2\,max}$ differ between control and HR mice; specifically, that selection for high voluntary wheel running

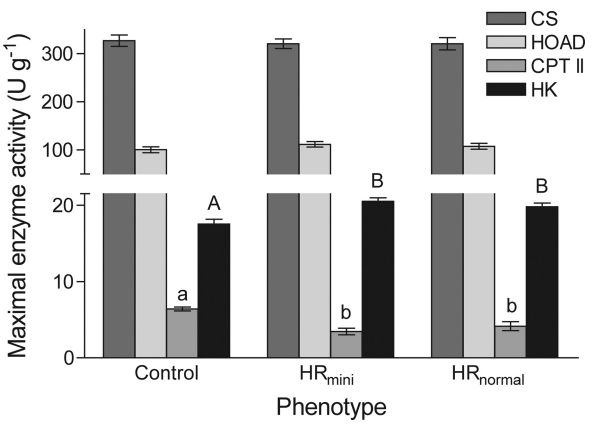

Fig. 3. Maximal enzyme activities (relative to g tissue wet weight) for citrate synthase (CS), β-hydroxyacyl-CoA dehydrogenase (HOAD), carnitine palmitoyltransferase (CPT) II, and hexokinase (HK) in the left ventricle of control mice and selectively bred HR_{mini} and HR_{normal} mice (n = 7–8). Data are presented as simple means ± SE. For each enzyme, the presence of letters denotes statistical significance, where bars not sharing a common letter are significantly different from each other ($P < 0.05$). U = μmol/min.

may have resulted in changes to central factors in the oxygen cascade, contributing to the increased aerobic capacity of HR mice (38, 39). As cardiac output is an important central component of oxygen delivery, we characterized some physical and metabolic properties of HR_{mini}, HR_{normal}, and control mouse hearts.

HR_{mini} mice have a significantly greater left ventricle mass and thus whole ventricular mass than both control and HR_{normal} mice, relative to body mass (Table 3), which is consistent with the findings of Rezende and colleagues (39). However, without body mass as a covariate, neither left nor whole ventricles are significantly larger in HR_{mini} mice, and left ventricles of all mouse phenotypes contain comparable levels of DNA (Table 3). Therefore, this difference in relative heart size could be viewed as predominately reflective of the reduced body masses of HR_{mini} mice as opposed to cardiac hypertrophy per se. However, relative heart mass can give a good indication of an animal's ability to perform sustained aerobic locomotion (4, 51), so it is likely that the increased ratio of heart to body size contributes to the elevated $\dot{V}O_{2\,max}$ of HR_{mini} mice.

Additionally, both phenotypes of HR mice show evidence of metabolic alterations in the left ventricle. Compared with control mice, HR mice show a reduction in the left ventricular maximal activity of CPT II, an enzyme in the fatty acid catabolic pathway (Fig. 3). Although a nonreversible switch in the basal-preferred fuel substrate from fatty acids to carbohydrates is often regarded as a deleterious hallmark of pressure- or volume-overloaded hypertrophic hearts (36), these mice show no statistically significant differences in ventricular mRNA levels of several genes involved in fatty acid catabolism, including *PPARα*, *MCAD*, and both muscle- and liver-type *CPT-1*. Therefore, it is unlikely that this reduced maximal activity of CPT II in HR left ventricles signifies a diminished capacity for fatty acid oxidation, particularly as there is no change in the maximal activity of HOAD, another fatty acid catabolic enzyme. There is, however, increased maximal activity of HK in the left ventricles of sedentary (i.e., not exercise trained) HR mice compared with control mice (Fig. 3). Upregulated HK is also characteristic of physiologically hypertrophic hearts in exercise-trained rats as a component of the elevated overall metabolic capacity (45). Therefore, differences between HR and control mouse cardiac metabolic enzyme activities may contribute to the enhancement of $\dot{V}O_{2\,max}$ and capacity for sustained aerobic exercise in HR mice in

Table 4. *mRNA expression in cardiac muscle of control, HR_{mini}, and HR_{normal} mice*

	Control Mice	HR_{mini} Mice	HR_{normal} Mice
PPARα relative mRNA			
Left ventricle	1.00 ± 0.18 (7)	0.78 ± 0.03 (7)	1.05 ± 0.14 (8)
Right ventricle	1.00 ± 0.09 (6)	0.88 ± 0.10 (7)	1.28 ± 0.20 (8)
MCAD relative mRNA			
Left ventricle	1.00 ± 0.13 (7)	0.99 ± 0.11 (7)	0.94 ± 0.13 (8)
Right ventricle	1.00 ± 0.14 (7)	0.94 ± 0.14 (8)	1.31 ± 0.23 (8)
CPT-1α relative mRNA			
Left ventricle	1.00 ± 0.22 (7)	0.74 ± 0.10 (7)	0.79 ± 0.10 (8)
Right ventricle	1.00 ± 0.17 (6)	0.92 ± 0.18 (7)	1.42 ± 0.32 (8)
CPT-1β relative mRNA			
Left ventricle	1.00 ± 0.17 (7)	0.86 ± 0.06 (7)	0.82 ± 0.06 (8)
Right ventricle	1.00 ± 0.09 (6)	0.88 ± 0.10 (7)	1.28 ± 0.20 (8)

Data are presented as simple means ± SE, with sample size shown in parenthesis; mRNA expression levels are corrected against *TBP* mRNA, and values are reported normalized to the mean control mouse value (arbitrarily set at 1.00). Statistical analyses were performed on raw mRNA levels corrected against *TBP* mRNA; no differences between groups were statistically significant. See text for definitions of abbreviations.

conjunction with the increased relative heart size of HR_{mini} mice.

Whole body fuel use during exercise. The mix of metabolic fuels used across two submaximal relative exercise intensities does not differ statistically among HR_{mini}, HR_{normal}, and control mice, when fuel oxidation rates are expressed as a percentage of total oxygen consumption (Fig. 2). Rather, HR mice exhibit greater rates of lipid oxidation (i.e., enhanced total lipid flux) than control mice during low-intensity exercise (66% $\dot{V}O_{2\,max}$), commensurate with their elevated $\dot{V}O_{2\,max}$ (Fig. 1, Table 2). When exercising at a higher intensity (78% $\dot{V}O_{2\,max}$), the increased energetic demand in all mice is supported by an elevated flux of carbohydrates, and the absolute rate of lipid oxidation in control mice matches the rates in HR mice (Table 2).

HR mice primarily achieve greater levels of voluntary wheel running by running faster than control mice on exercise wheels (13–15, 17, 46). Our findings suggest that due to an increased aerobic capacity, HR mice are able to run at these faster speeds predominately sustained by lipid oxidation, whereas mice from nonselected control lines would require a higher proportion of carbohydrates to achieve equivalent absolute exercise intensities. Therefore, an enhanced capacity for absolute lipid oxidation in conjunction with an increased $\dot{V}O_{2\,max}$ may have enabled the shift in locomotor speed preference in HR mice, thus allowing them to achieve the greater levels of voluntary exercise for which they are selectively bred (see also Ref. 41). In fact, consumption of a high-fat diet further increases the amount of voluntary wheel running performed by HR (but not control) mice (33). Interestingly, rats from a line selectively bred for high treadmill endurance capacity with an elevated $\dot{V}O_{2\,max}$ exhibit greater in vitro skeletal muscle palmitate oxidation rates compared with a line selected for low endurance capacity (23, 26), signifying that increased lipid oxidation capacity is a common result of selection for running capacity.

Roberts et al. (41) and McClelland (29) have suggested that conserved mammalian fuel-use patterns are the result of the progression of muscle fiber recruitment, with the increasing proportionate reliance on carbohydrates at higher exercise intensities corresponding to the recruitment of fast glycolytic muscle fibers among all mammals (25, 44). Intriguingly, HR_{mini} mice do not have a large quantity of type IIB (fast glycolytic) fibers available for recruitment in their reduced-size hindlimb muscles (3, 18, 19), and yet they exhibit the ability to reach a whole body rate of carbohydrate combustion that is equivalent to mice with the normal muscle phenotype, at least under the submaximal exercise conditions tested here. Moreover, as the proportional reliance on carbohydrates for total oxidation at higher exercise intensities is comparable between HR_{mini} mice and HR_{normal} mice, it may be possible for mammals to differ in muscle fiber recruitment patterns during exercise without deviating from a conserved whole body pattern of proportionate fuel mix.

From these findings, we investigated other potential regulators of metabolic fuel use to determine whether phenotypically divergent HR mice might utilize different strategies to adjust substrate flux. Specifically, we focused here on several regulators of fatty acid uptake and catabolism in the skeletal muscle, in keeping with our stated hypothesis. However, future studies should explore other pathways (see Refs. 29 and 50), such as carbohydrate or amino acid metabolism or lactate clearance capacity, to further delineate different mechanisms regulating all of the fuels available to power exercise in mammals.

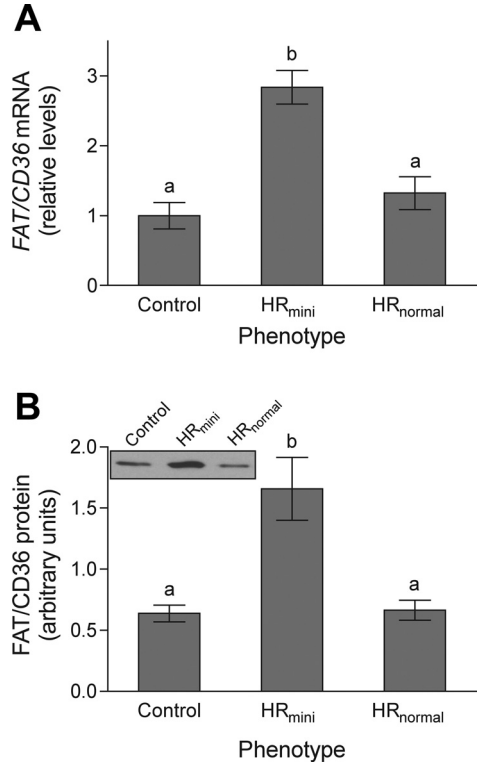

Fig. 4. Cellular mRNA levels of *FAT/CD36* (*A*) and sarcolemmal FAT/CD36 protein content (*B*) in the gastrocnemius of control mice and selectively bred HR_{mini} and HR_{normal} mice (n = 6–10). mRNA levels are expressed corrected against *18S* mRNA and normalized to the mean control mouse value (arbitrarily set at a value of 1.0). Statistical analyses for gene expression were performed on raw mRNA levels corrected against *18S* mRNA. Protein levels are expressed relative to a mixed standard sample, in arbitrary units. *Inset* in *B* shows a single representative immunoblot of sarcolemmal FAT/CD36 in control, HR_{mini}, and HR_{normal} mice, respectively (5 μg total protein loaded per gel lane). All data are presented as simple means ± SE. Bars not sharing a common letter are significantly different from each other ($P < 0.05$).

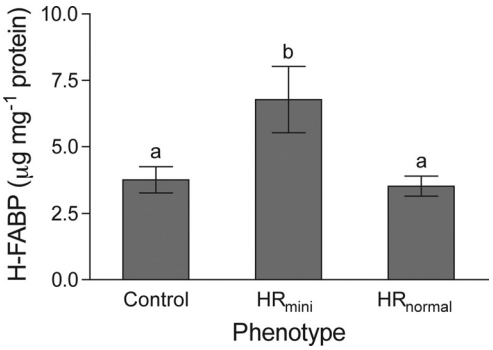

Fig. 5. Cytosolic heart-type fatty acid binding protein (H-FABP) protein content (relative to mg of total cytosolic protein) in the gastrocnemius of control mice and selectively bred HR_{mini} and HR_{normal} mice (n = 8–9). Data are presented as simple means ± SE. Bars not sharing a common letter are significantly different from each other ($P < 0.05$).

Capacity for circulatory fuel uptake into working muscle. FAT/CD36 is a pivotal sarcolemmal transporter of long-chain fatty acids, and its overexpression can lead to elevated fatty acid oxidation, as well as increased rates of fatty acid transport into giant sarcolemmal vesicles (35). Both cellular mRNA expression and sarcolemmal protein content of FAT/CD36 is substantially augmented in the gastrocnemius muscle of HR_{mini} mice compared with HR_{normal} or control mice (Fig. 4), which suggests that the mini muscles of HR_{mini} mice may have an enhanced capacity for uptake of circulatory fatty acids. Furthermore, the gastrocnemius of HR_{mini} mice exhibit an 80% higher cytosolic content of H-FABP (Fig. 5), a protein that serves as an intracellular sink for fatty acids transported across the sarcolemma, and enables their movement through the cytoplasm (16). Although it seems that H-FABP is not a direct regulator of fatty acid translocation across the sarcolemma, increased H-FABP levels could accommodate rapid changes in substrate flux, such as during the transition from resting to contracting muscle (27). Interestingly, despite these innate biochemical differences in the skeletal muscle, our in vivo results suggest that HR_{mini} mice do not have (or do not capitalize upon) an enhanced whole body capacity to utilize lipids during high-intensity exercise compared with mice with the normal muscle phenotype. Perhaps the muscle phenotype

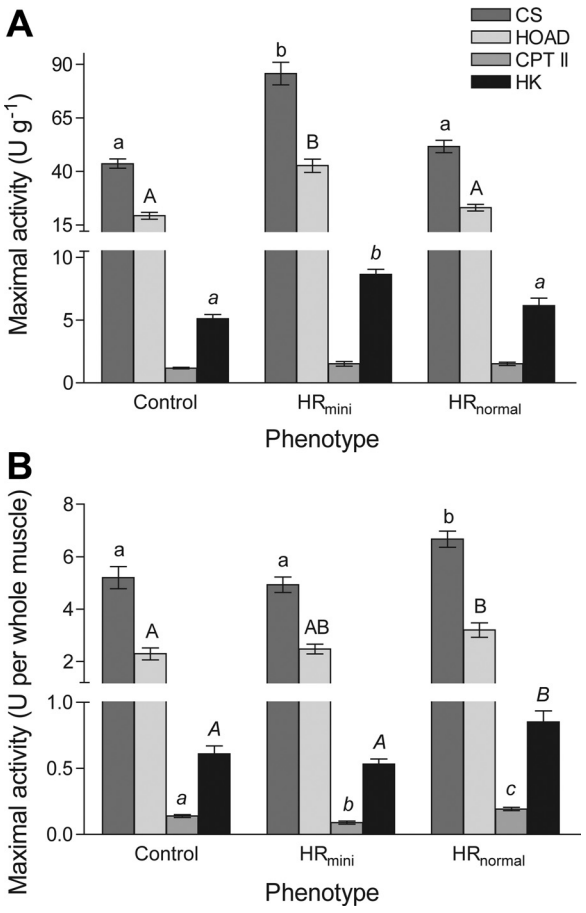

Fig. 6. Maximal enzyme activities for citrate synthase (CS), β-hydroxyacyl-CoA dehydrogenase (HOAD), carnitine palmitoyltransferase (CPT) II, and hexokinase (HK) in the gastrocnemius of control mice and selectively bred HR_{mini} and HR_{normal} mice (n = 7–10), expressed relative to g tissue wet mass (*A*) or per whole muscle mass (*B*). Data are presented as simple means ± SE. For each enzyme, the presence of letters denotes statistical significance, where bars not sharing a common letter are significantly different from each other ($P < 0.05$). U = μmol/min.

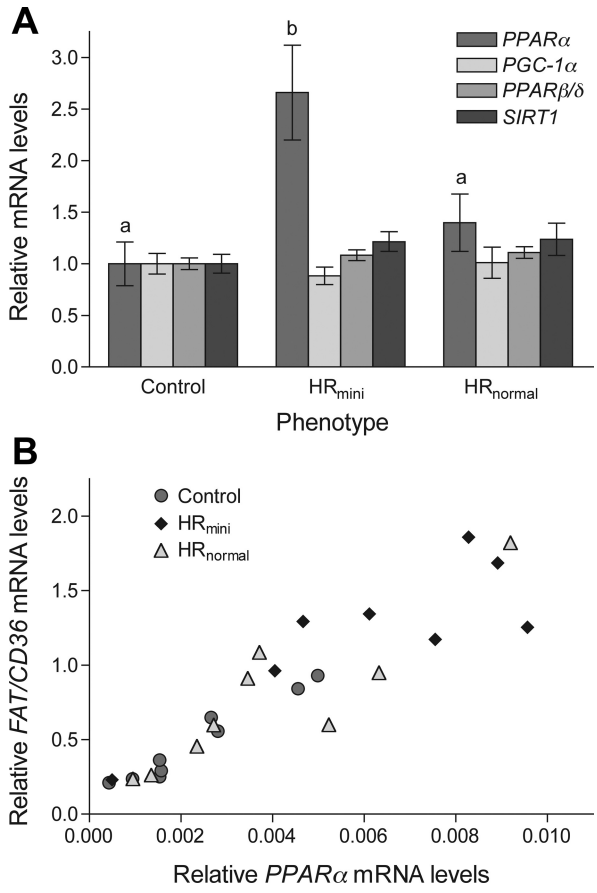

Fig. 7. Relative gene expression of transcriptional factors in the gastrocnemius of control mice and selectively bred HR_{mini} and HR_{normal} mice (n = 7–9). *A*: mRNA levels of *PPARα*, *PGC-1α*, *PPARβ/δ*, and *SIRT1* are expressed corrected against *18S* mRNA and normalized to the mean control mouse value (arbitrarily set at a value of 1.0). Data are presented as simple means ± SE. Statistical analyses were performed on raw mRNA levels corrected against *18S* mRNA; for each gene, the presence of letters denotes statistical significance, where mouse phenotypes not sharing a common letter are significantly different from each other ($P < 0.05$). *B*: relationship between the transcript levels of *PPARα* and *FAT/CD36*, where mRNA levels of individual mice are expressed corrected against *18S*. For this correlation, $r = 0.92$, $P \leq 0.001$.

differences reflect more an increased reliance on circulatory versus intramuscular lipids in the HR_{mini} line.

HR_{mini} mice may also have an enhanced capacity for utilizing circulatory glucose in working muscle. During exercise, when the glucose transporter GLUT-4 has been translocated to the plasma membrane, the phosphorylation of glucose by HK becomes a significant functional barrier of glucose uptake into the myocyte (see Ref. 49). While it has previously been shown that there are no differences in constitutive GLUT-4 levels in the gastrocnemius of resting HR_{mini}, HR_{normal}, or control mice, when housed without access to running wheels (17), HR_{mini} mice do have increased mass-specific maximal HK activity in the gastrocnemius (Fig. 6). This elevated HK activity may facilitate enhanced glucose uptake into the gastrocnemius during exercise (see also Refs. 3, 18, 22), given that transgenic mice overexpressing HK II show increased glucose uptake into skeletal muscle during moderate-intensity exercise (20). Indeed, before exercise, HR_{mini} mice have larger liver glycogen depots than the other mouse phenotypes (17), and liver glycogen is an important source of energy during exercise for rodents (2).

Although these data point to variation in the capacity for utilizing circulatory fuels, since neither postexercise intramuscular substrate depletions nor in vivo muscle uptake rates for circulatory fuels during locomotion were measured in these mice, further inferences are limited by the complexities of fuel metabolism.

Skeletal muscle capacity for oxidative metabolism. The increased capacity for substrate uptake into the skeletal muscle of HR_{mini} mice is accompanied by an enhanced mass-specific capacity to utilize fatty acids. In addition to the increased mass-specific maximal activities of CS, which is a hallmark of the "mini muscle" phenotype's enhanced aerobic capacity (18, 22), we show that sedentary HR_{mini} mice also have an enhanced capacity for β-oxidation at the level of HOAD specific activity in the gastrocnemius (Fig. 6).

On a whole muscle basis, HR_{mini} mice tend to have equivalent maximal enzyme activities as control mice (see also Ref. 22). Conversely, HR_{normal} mice (at least the line sampled here) appear to exhibit an enhancement of the overall metabolic capacity of the gastrocnemius. Because of the slight (but statistically nonsignificant) muscle enlargement compared with control mice, HR_{normal} mice have significantly greater whole muscle maximal activities of CS, HOAD, CPT II, and HK than control mice (and HR_{mini} mice, with the exception of HOAD; Fig. 6). Having a bigger muscle mass as opposed to greater mass-specific activities of metabolic enzymes may be a distinct mechanism that help HR_{normal} mice achieve elevated whole body fuel oxidation rates (compared with control mice), commensurate with their increased $\dot{V}O_{2\,max}$.

Transcriptional regulation of skeletal muscles properties. Constitutive gene expression of *PGC-1α*, *PPARβ/δ*, and *SIRT1* in muscle are not significantly different among HR_{mini}, HR_{normal}, and control mice (Fig. 7), suggesting that these transcription factors do not play a major role in the distinct properties of the "mini muscle." However, HR_{mini} mice do exhibit greatly enhanced *PPARα* mRNA expression in the gastrocnemius, and this may be an underlying basis for many of the altered metabolic characteristics of this skeletal muscle. PPARα is one of the most predominant PPAR isoforms in skeletal muscle, and it is involved in the upregulation of many genes in the fatty acid metabolic pathway (29). For instance, our results show a strong correlation between mRNA levels of *PPARα* and *FAT/CD36* among all mice, which suggests a close relationship between the transcript levels of this transcription factor and a target gene (Fig. 7).

Perspectives and Significance

Despite divergent patterns in daily locomotor behavior and aerobic capacity, the proportionate mix of fuels used across relative exercise intensities was not statistically different for HR_{mini}, HR_{normal}, and control mice. Instead, this experimental evolution model supports the results of interspecific comparative studies (29, 41, 50) and shows that absolute rates of fuel use during submaximal exercise scale with variation in aerobic capacity among diverse mammals. Furthermore, owing to substantial differences in muscle anatomy and biochemistry, the HR mouse model demonstrates that it may be possible for mammals to differ in muscle fiber recruitment patterns while maintaining a conserved whole body pattern of fuel use, thus emphasizing the robustness of the mammalian fuel use pattern. Based on our findings, we propose that aerobic capacity and locomotor behavior may be evolutionary linked to the capacity for lipid oxidation. Through the course of evolution, mammals may exhibit multiple potential mechanisms or "solutions" [sensu Garland et al. (14)] to enhance lipid oxidation rates commensurate with aerobic capacity; biochemical traits can therefore differ between genetically or phenotypically distinct mammals without causing deviation from a conserved whole body fuel-use pattern.

ACKNOWLEDGMENTS

Financial support was provided by a Natural Science and Engineering Council of Canada (NSERC) Discovery Grant to G. B. McClelland and National Science Foundation (NSF) grants to T. Garland (IOS-1121273). G. B. McClelland is also the recipient of an Early Researcher Award from the Ontario Ministry of Research and Innovation. N. M. Templeman was supported by a NSERC Canada Graduate Scholarship and by a Journal of Experimental Biology Travelling Fellowship. H. Schutz was a Chancellor's Postdoctoral Fellow at University of California, Riverside.

DISCLOSURES

No conflicts of interest, financial or otherwise, are declared by the author(s).

AUTHOR CONTRIBUTIONS

Author contributions: N.M.T., T.G., and G.B.M. conception and design of research; N.M.T. and H.S. performed experiments; N.M.T., H.S., and T.G. analyzed data; N.M.T., T.G., and G.B.M. interpreted results of experiments; N.M.T. prepared figures; N.M.T. drafted manuscript; N.M.T., H.S., T.G., and G.B.M. edited and revised manuscript; N.M.T., H.S., T.G., and G.B.M. approved final version of manuscript.

REFERENCES

1. **Asher G, Gatfield D, Stratmann M, Reinke H, Dibner C, Kreppel F, Mostoslavsky R, Alt FW, Schibler U.** SIRT1 regulates circadian clock gene expression through PER2 deacetylation. *Cell* 134: 317–328, 2008.
2. **Baldwin K, Reitman J, Terjung R, Winder W, Holloszy J.** Substrate depletion in different types of muscle and in liver during prolonged running. *Am J Physiol* 225: 1045–1050, 1973.
3. **Bilodeau GM, Guderley H, Joanisse DR, Garland T Jr.** Reduction of type IIb myosin and IIB fibers in tibialis anterior muscle of mini-muscle mice from high-activity lines. *J Exp Zool A* 311A: 189–198, 2009.
4. **Bishop CM.** Heart mass and the maximum cardiac output of birds and mammals: implications for estimating the maximum aerobic power input of flying animals. *Philos Trans R Soc Lond B Biol Sci* 352: 447–456, 1997.

5. **Brooks GA, Mercier J.** Balance of carbohydrate and lipid utilization during exercise: the "crossover" concept. *J Appl Physiol* 76: 2253–2261, 1994.
6. **Brooks GA.** Mammalian fuel utilization during sustained exercise. *Comp Biochem Physiol B Biochem Mol Biol* 120: 89–107, 1998.
7. **Butz CE, McClelland GB, Brooks GA.** MCT1 confirmed in rat striated muscle mitochondria. *J Appl Physiol* 97: 1059–1066, 2004.
8. **Cikos S, Bukovska A, Koppel J.** Relative quantification of mRNA: comparison of methods currently used for real-time PCR data analysis. *BMC Mol Biol* 8: 113, 2007.
9. **Edwards HT, Margaria R, Dill DB.** Metabolic rate, blood sugar and the utilization of carbohydrate. *Am J Physiol* 108: 203–209, 1934.
10. **Felig P, Wahren J.** Fuel homeostasis in exercise. *N Engl J Med* 293: 1078–1084, 1975.
11. **Frayn KN.** Calculation of substrate oxidation rates in vivo from gaseous exchange. *J Appl Physiol* 55: 628–634, 1983.
12. **Garland T Jr.** Selection experiments: an under-utilized tool in biomechanics and organismal biology. In: *Vertebrate Biomechanics And Evolution*, edited by Bels VL, Gasc JP, Casinos A. Oxford: BIOS Scientific, 2003, p. 23–56.
13. **Garland T Jr, Morgan MT, Swallow JG, Rhodes JS, Girard I, Belter JG, Carter PA, Cheverud J.** Evolution of a small-muscle polymorphism in lines of house mice selected for high activity levels. *Evolution* 56: 1267–1275, 2002.
14. **Garland TJr, Kelly SA, Malisch JL, Kolb EM, Hannon RM, Keeney BK, Van Cleave SL, Middleton KM.** How to run far: multiple solutions and sex-specific responses to selective breeding for high voluntary activity levels. *Proc Biol Sci* 278: 574–582, 2011.
15. **Girard I, McAleer MW, Rhodes JS, Garland T Jr.** Selection for high voluntary wheel-running increases speed and intermittency in house mice (*Mus domesticus*). *J Exp Biol* 204: 4311–4320, 2001.
16. **Glatz JFC, Schaap FG, Binas B, Bonen A, van der Vusse GJ, Luiken JJFP.** Cytoplasmic fatty acid-binding protein facilitates fatty acid utilization by skeletal muscle. *Acta Physiol Scand* 178: 367–371, 2003.
17. **Gomes FR, Rezende EL, Malisch JL, Lee SK, Rivas DA, Kelly SA, Lytle C, Yaspelkis BB, III, Garland T Jr.** Glycogen storage and muscle glucose transporters (GLUT-4) of mice selectively bred for high voluntary wheel running. *J Exp Biol* 212: 238–248, 2009.
18. **Guderley H, Houle-Leroy P, Diffee GM, Camp DM, Garland T Jr.** Morphometry, ultrastructure, myosin isoforms, and metabolic capacities of the "mini muscles" favoured by selection for high activity in house mice. *Comp Biochem Physiol B Biochem Mol Biol* 144: 271–282, 2006.
19. **Guderley H, Joanisse DR, Mokas S, Bilodeau GM, Garland T Jr.** Altered fibre types in gastrocnemius muscle of high wheel-running selected mice with mini-muscle phenotypes. *Comp Biochem Physiol B Biochem Mol Biol* 149: 490–500, 2008.
20. **Halseth AE, Bracy DP, Wasserman DH.** Overexpression of hexokinase II increases insulin and exercise-stimulated muscle glucose uptake in vivo. *Am J Physiol Endocrinol Metab* 276: E70–E77, 1999.
21. **Houle-Leroy P, Garland T Jr, Swallow JG, Guderley H.** Effects of voluntary activity and genetic selection on muscle metabolic capacities in house mice *Mus domesticus*. *J Appl Physiol* 89: 1608–1616, 2000.
22. **Houle-Leroy P, Guderley H, Swallow JG, Garland T Jr.** Artificial selection for high activity favors mighty mini-muscles in house mice. *Am J Physiol Regul Integr Comp Physiol* 284: R433–R443, 2003.
23. **Howlett RA, Kirkton SD, Gonzalez NC, Wagner HE, Britton SL, Koch LG, Wagner PD.** Peripheral oxygen transport and utilization in rats following continued selective breeding for endurance running capacity. *J Appl Physiol* 106: 1819–1825, 2009.
24. **Kolb EM, Kelly SA, Middleton KM, Sermsakdi LS, Chappell MA, Garland T.** Erythropoietin elevates VO_{2max} but not voluntary wheel running in mice. *J Exp Biol* 213: 510–519, 2010.
25. **Laughlin MH, Armstrong RB.** Muscular blood flow distribution patterns as a function of running speed in rats. *Am J Physiol Heart Circ Physiol* 243: H296–H306, 1982.
26. **Lessard SJ, Rivas DA, Stephenson EJ, Yaspelkis BB, Koch LG, Britton SL, Hawley JA.** Exercise training reverses impaired skeletal muscle metabolism induced by artificial selection for low aerobic capacity. *Am J Physiol Regul Integr Comp Physiol* 300: R175–R182, 2011.
27. **Luiken J, Koonen D, Coumans W, Pelsers M, Binas B, Bonen A, Glatz J.** Long-chain fatty acid uptake by skeletal muscle is impaired in homozygous, but not heterozygous, heart-type-FABP null mice. *Lipids* 38: 491–496, 2003.
28. **McClelland GB, Kraft CS, Michaud D, Russell JC, Mueller CR, Moyes CD.** Leptin and the control of respiratory gene expression in muscle. *Biochim Biophys Acta Mol Cell Biol Lipids* 1688: 86–93, 2004.
29. **McClelland GB.** Fat to the fire: the regulation of lipid oxidation with exercise and environmental stress. *Comp Biochem Physiol B Biochem Mol Biol* 139: 443–460, 2004.
30. **McClelland GB, Brooks GA.** Changes in MCT 1, MCT 4, and LDH expression are tissue specific in rats after long-term hypobaric hypoxia. *J Appl Physiol* 92: 1573–1584, 2002.
31. **McClelland GB, Hochachka PW, Weber JM.** Carbohydrate utilization during exercise after high-altitude acclimation: A new perspective. *Proc Natl Acad Sci USA* 95: 10288–10293, 1998.
32. **McGarry JD, Sen A, Esser V, Woeltje KF, Weis B, Foster DW.** New insights into the mitochondrial carnitine palmitoyltransferase enzyme system. *Biochimie* 73: 77–84, 1991.
33. **Meek TH, Eisenmann JC, Garland T.** Western diet increases wheel running in mice selectively bred for high voluntary wheel running. *Int J Obes* 34: 960–969, 2010.
34. **Meek TH, Lonquich BP, Hannon RM, Garland T Jr.** Endurance capacity of mice selectively bred for high voluntary wheel running. *J Exp Biol* 212: 2908–2917, 2009.
35. **Nickerson JG, Alkhateeb H, Benton CR, Lally J, Nickerson J, Han X, Wilson MH, Jain SS, Snook LA, Glatz JFC, Chabowski A, Luiken JJFP, Bonen A.** Greater transport efficiencies of the membrane fatty acid transporters FAT/CD36 and FATP4 compared with FABPpm and FATP1 and differential effects on fatty acid esterification and oxidation in rat skeletal muscle. *J Biol Chem* 284: 16522–16530, 2009.
36. **Rajabi M, Kassiotis C, Razeghi P, Taegtmeyer H.** Return to the fetal gene program protects the stressed heart: a strong hypothesis. *Heart Fail Rev* 12: 331–343, 2007.
37. **Rennie MJ, Edwards RHT, Halliday D, Davies CTM, Matthews DE, Millward DJ.** Protein metabolism during exercise. In: *Nitrogen Metabolism in Man*, edited by Waterlow JC, Stephen JML. London: Applied Science, 1981, p. 509–523.
38. **Rezende EL, Garland T Jr, Chappell MA, Malisch JL, Gomes FR.** Maximum aerobic performance in lines of *Mus* selected for high wheel-running activity: effects of selection, oxygen availability and the mini-muscle phenotype. *J Exp Biol* 209: 115–127, 2006.
39. **Rezende EL, Gomes FR, Malisch JL, Chappell MA, Garland T Jr.** Maximal oxygen consumption in relation to subordinate traits in lines of house mice selectively bred for high voluntary wheel running. *J Appl Physiol* 101: 477–485, 2006.
40. **Rezende E, Kelly S, Gomes F, Chappell M, Garland T Jr.** Effects of size, sex, and voluntary running speeds on costs of locomotion in lines of laboratory mice selectively bred for high wheel-running activity. *Physiol Biochem Zool* 79: 83–99, 2006.
41. **Roberts TJ, Weber JM, Hoppeler H, Weibel ER, Taylor CR.** Design of the oxygen and substrate pathways. II: Defining the upper limits of carbohydrate and fat oxidation. *J Exp Biol* 199: 1651–1658, 1996.
42. **Romijn JA, Coyle EF, Sidossis LS, Gastaldelli A, Horowitz JF, Endert E, Wolfe RR.** Regulation of endogenous fat and carbohydrate metabolism in relation to exercise intensity and duration. *Am J Physiol Endocrinol Metab* 265: E380–E391, 1993.
43. **Seeherman HJ, Richard Taylor C, Maloiy GMO, Armstrong RB.** Design of the mammalian respiratory system. II: Measuring maximum aerobic capacity. *Respir Physiol* 44: 11–23, 1981.
44. **Smith JL, Edgerton VR, Betts B, Collatos TC.** EMG of slow and fast ankle extensors of cat during posture, locomotion, and jumping. *J Neurophysiol* 40: 503–513, 1977.
45. **Strøm CC, Aplin M, Ploug T, Christoffersen TEH, Langfort J, Viese M, Galbo H, Haunsø S, Sheikh SP.** Expression profiling reveals differences in metabolic gene expression between exercise-induced cardiac effects and maladaptive cardiac hypertrophy. *FEBS J* 272: 2684–2695, 2005.
46. **Swallow JG, Carter PA, Garland T.** Artificial selection for increased wheel-running behavior in house mice. *Behav Genet* 28: 227–237, 1998.
47. **Swallow JG, Garland T Jr, Carter PA, Zhan W, Sieck GC.** Effects of voluntary activity and genetic selection on aerobic capacity in house mice (*Mus domesticus*). *J Appl Physiol* 84: 69–76, 1998.
48. **Templeman NM, Beaudry JL, Le Moine CMR, McClelland GB.** Chronic hypoxia- and cold-induced changes in cardiac enzyme and gene expression in CD-1 mice. *Biochim Biophys Acta Gen Subj* 1800: 1248–1255, 2010.

49. **Wasserman DH, Kang L, Ayala JE, Fueger PT, Lee-Young RS.** The physiological regulation of glucose flux into muscle in vivo. *J Exp Biol* 214: 254–262, 2011.
50. **Weber JM, Haman F.** Oxidative fuel selection: adjusting mix and flux to stay alive. *Int Congr* 1275: 22–31, 2004.
51. **Weibel ER, Bacigalupe LD, Schmitt B, Hoppeler H.** Allometric scaling of maximal metabolic rate in mammals: muscle aerobic capacity as determinant factor. *Respir Physiol Neurobiol* 140: 115–132, 2004.
52. **Withers PC.** Measurement of VO_2, VCO_2, and evaporative water loss with a flow-through mask. *J Appl Physiol* 42: 120–123, 1977.